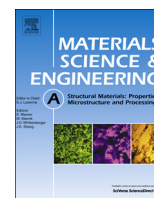




ELSEVIER

Contents lists available at ScienceDirect

## Materials Science &amp; Engineering A

journal homepage: [www.elsevier.com/locate/msea](http://www.elsevier.com/locate/msea)

# Creep behaviors and role of dislocation network in a powder metallurgy Ni-based superalloy during medium-temperature

Jun Xie<sup>a</sup>, Sugui Tian<sup>a</sup>, Li Juan Shang<sup>a</sup>, Xiaoming Zhou<sup>b</sup>

<sup>a</sup> School of Materials Science and Engineering, Shenyang University of Technology, Shenyang 110870, China

<sup>b</sup> Beijing Institute of Aeronautical Materials, National Key Laboratory for Advanced High Temperature Structural Materials, Beijing 100095, China

## ARTICLE INFO

## Article history:

Received 8 October 2013

Received in revised form

25 January 2014

Accepted 24 March 2014

Available online 30 March 2014

## Keywords:

FGH95 powder metallurgy Ni-base

superalloy

Creep

Deformation mechanism

Dislocation reaction

Dislocation networks

## ABSTRACT

By means of creep properties measurement, microstructure observation and contrast analysis of dislocation configuration, the creep behaviors and role of dislocation networks in FGH95 powder metallurgy Ni-based superalloy during creep have been investigated. The results show that the microstructure of alloy consists of the fine  $\gamma'$  phase coherently embedded in the  $\gamma$  matrix, and a few coarser  $\gamma'$  particles are distributed in the boundary regions. In the ranges of the applied temperatures and stresses, the alloy displays a better creep resistance and longer lifetime. The deformation mechanisms of alloy during creep are the dislocations slipping in the matrix and shearing into the  $\gamma'$  phase, and the dislocations shearing into the  $\gamma'$  phase may be decomposed to form the configuration of the partials plus the stacking fault. During creep, two groups of dislocations on different slip planes may knit to form the quadrangular dislocation networks; while two groups of moving dislocations on the same slip plane may encounter and react to form the hexagonal dislocation networks. The strength of boundaries is responsible for the creep resistance of alloy, and the one is related to the deforming behaviors of coarse  $\gamma'$  particles distributed in the boundaries. Thereinto, the dislocation networks distributed in the interfaces of coarse  $\gamma'/\gamma$  phases may release the lattice-misfit stress and relax the stress concentration to delay the dislocation shearing into the  $\gamma'$  phase, which is beneficial to keep the boundary strength and enhance the creep resistance of the alloy.

© 2014 Elsevier B.V. All rights reserved.

## 1. Introduction

Powder metallurgy (P/M) Ni-based superalloys are an excellent material used for preparing the high temperature rotating parts of the advanced aero-engines due to their excellent comprehensive properties, such as no macro-segregation, high yield strength and good fatigue tolerance [1,2]. Especially, FGH95 superalloy has a high volume fraction of  $\gamma'$  phase (about 50%), and excellent integrating mechanical properties at 650 °C [3–5]; therefore, they are and mainly used for preparing the turbine disk parts of the advanced aero-engines [6–9]. The microstructure of FGH95 (René 95) P/M Ni-base superalloy consists of  $\gamma$  matrix and  $\gamma'$  phase [10,11], and the morphology and distribution of the  $\gamma'$  phase are related to the preparation of technologies of the one, which has an important effect on the mechanical and creep properties of the alloy. During creep, the deformation mechanisms in Ni-base superalloy depend on the alloy chemistry, morphology and volume fraction of  $\gamma'$  phase and service conditions [12–14]. Thereinto, the creep mechanisms of the alloy include the formation of the anti-phase boundary (APB), dislocations slipping in  $\gamma$  matrix and shearing or bypassing  $\gamma'$  phase, and micro-twinning deformation [15–17]. Moreover, the dislocation networks may be formed in the  $\gamma/\gamma'$  interface of Ni-based superalloy, which may release the

stress of lattice mismatch to improve the stability of the microstructure and enhance the creep resistance of the alloy [18–20].

The preparation process of FGH95 alloy includes the powder pre-treatment, hot isostatic pressing (HIP) and heat treatments. The heat treatments of FGH95 alloy mainly include high temperature solution and aging [21,22]; after solution treatment the alloy may be quenched in different mediums, such as “oil bath” or “molten salt bath”. During creep, the deformation mechanism of the alloy cooled in oil bath is the double orientations slipping of dislocations in the matrix, and the  $\gamma'$ -free phase zones near the boundaries which are broken into irregular piece-like shapes due to the severe plastic deformation [23]. While the deformed features of the alloy treated in molten salt are that the twinning and dislocation slipping are activated in the matrix, thereinto, the particle-like carbides are dispersedly precipitated within the grains and along the boundary, which may effectively restrain the dislocation slipping to improve the creep resistance of the alloy [24]. Moreover, the dislocation networks may be formed in the matrix of the alloy quenched in molten salt bath, which may decrease the strain rate during steady state creep to prolong the creep lifetime of the alloy [25]. Although the creep mechanisms of FGH95 PM Ni-base superalloy have been reported [26,27], the formation and the effect of dislocation networks in the PM Ni-base superalloy during creep are still unclear.

**Table 1**  
Chemical composition of FGH95 powder Nickel based superalloy (mass fraction, %)

C	B	Cr	Co	Al	Ti	W	Mo	Nb	Ni
0.060	0.012	12.98	8.00	3.48	2.55	3.40	3.40	3.50	Bal.

Hereby, after heat treatment the creep property of FGH95 P/M Ni-base superalloy is measured under experiment conditions, and the microstructures of the alloy crept for different times are observed by transmission electron microscopy (TEM) for investigating the formation and effect of dislocation network in FGH95 PM Ni-base superalloy during creep.

## 2. Experimental procedure

The powder particles of FGH95 (René 95) Ni-base superalloy with 150 meshes in size are put into a stainless steel can for pre-treating, at 1050 °C for 4 h, to degas and evacuate the process of the powders. And then the can containing FGH95 powder particles is hot isostatically pressed (HIP) for 4 h under the conditions of 1120 °C and 120 MPa to prepare the ingot of alloy. The chemical composition of FGH95 alloy is shown in Table 1. And the full heat treatment regime of the alloy is shown as follows: 1155 °C × 1 h (solution treatment)+550 °C × 15 min (cooling in molten salt bath)+870 °C × 1 h (primary aging treatment)+650 °C × 24 h (secondary aging treatment). And the cooling rates of the alloy quenched in molten salt bath are measured to be 150 °C/min. The error range of heat treatment furnace is about ± 2 °C.

After full heat treatment, the ingot of FGH95 superalloy is cut into the specimens with the cross-section of 4.5 mm × 2.5 mm and the gauge length of 20 mm. Uniaxial constant load tensile testing is performed, in a GW504 model creep testing machine, for measuring creep curves under the condition of 1034–1055 MPa and 650–670 °C. In order to study the formation and effect of dislocation networks during creep, the creep tests of alloy are interrupted after crept for 10, 40, and 100 h, and cooled down to room temperature under loading to keep the dislocation structure of the specimen. After crept for different times, the samples were cut into flakes and mechanically thinned down to about 50 μm in thickness to prepare the foils for TEM observation, and the TEM foils were electrochemically thinned in a solution of 7% perchloric acid in volume fraction and 93% ethanol at –25 °C. By means of the systematic tilting technology, the dislocation configurations in the alloy during creep were observed by TECNAI-20 transmission electron microscopy (TEM).

## 3. Experimental results and analysis

### 3.1. Creep curves of alloy

The creep curves of the alloy after heat treatment under different conditions are measured, as shown in Fig. 1. Thereinto, the creep curves of alloy under the applied different stresses at 650 °C are shown in Fig. 1(a); it is indicated that the creep lifetimes of the alloy under the applied stress of 1034 MPa, 1050 MPa and 1055 MPa are measured to be 283 h, 98 h and 58 h, respectively, as marked by the numbers 1, 2 and 3 in Fig. 1(a). Especially, the creep lifetimes of alloy decrease from 283 h to 98 h when the applied stress enhances from 1034 MPa to 1050 MPa at 650 °C; the decreasing extent of the lifetime is about 180%, which indicates that the alloy has an obvious sensitivity to the applied stress when the applied stress is much more than 1034 MPa at 650 °C.

Under the applied stress of 1034 MPa at different temperatures, the creep curves of alloy are measured as shown in Fig. 1(b); thereinto, the creep curves of alloy measured under applied temperatures of 650 °C, 660 °C and 670 °C are marked by the numbers 1, 2, and 3 in Fig. 1(b) respectively. It is indicated that the strain rates of the alloy during steady state creep are measured to be 0.00184%/h, 0.00444%/h and 0.01051%/h under applied temperatures of 650 °C, 660 °C and 670 °C, respectively, which corresponds to the creep curves 1, 2 and 3 in Fig. 1(b), and the creep lifetimes of the alloy are measured to be 283 h, 139 h and 44 h, respectively. This indicates that the alloy has an obvious sensitivity to the applied temperature when the creep temperature is much more than 650 °C under the applied stress of 1034 MPa.

The transient strain of the alloy occurs at the moment of applying the load at high temperatures; significant amount of dislocations are activated for slipping in the alloy as the creep goes on, and the density of the dislocations increases to decrease the strain rate due to the effect of the strain hardening. The strain rate of the alloy remains constant once the creep of the alloy enters the steady state stage, and the strain rate of the alloy during steady state creep may be expressed by the Dorn law which is given as

$$\dot{\epsilon}_{ss} = A \sigma_A^n \exp\left(-\frac{Q}{RT}\right) \quad (1)$$

where  $\dot{\epsilon}_{ss}$  is the strain rate during steady state creep,  $A$  is a constant related to the microstructure,  $\sigma_A$  is the applied stress,  $n$  is the apparent stress exponent,  $R$  is the gas constant,  $T$  is the absolute temperature, and  $Q$  is the apparent creep activation energy.

According to the creep data in Fig. 1, in the ranges of the applied temperatures and stresses, the strain rate of the alloy during steady state creep is measured, and then the dependence of the strain rates of the alloy on the applied temperatures and stresses are expressed as  $(\ln \dot{\epsilon}_{ss} - 1/T)$  and  $(\ln \dot{\epsilon}_{ss} - \ln \sigma_A)$ , as shown in Fig. 2(a) and (b), respectively. Therefore, the apparent creep activation energy and stress exponent of the alloy during steady state creep may be determined to be  $Q=630.4 \pm 20$  kJ/mol and  $n=12.7$ , respectively. According to the stress exponent, it may be deduced that the dislocations slipping and shearing into  $\gamma'$  phase dominate the strain rate of the alloy during steady state creep.

### 3.2. Deformed features of alloy during creep

After heat treatment, the microstructure of the alloy is shown in Fig. 3, which indicates that the microstructure of alloy consists of the  $\gamma$  matrix, fine and coarser  $\gamma'$  phase, a few coarser  $\gamma'$  phase about 1–2 μm in size are distributed in the boundaries regions, as marked by the arrow in Fig. 3(a); the fine  $\gamma'$  particles about 0.1–0.2 μm in size are distributed dispersedly within the grains, as shown in Fig. 3(b). By means of the anode selective dissolving method and granularity analysis, the volume fraction of  $\gamma'$  phase in the FGH95 alloy is measured to be about 47%, the one of the coarser  $\gamma'$  phase is about 5.1% and the one of fine  $\gamma'$  phase is about 41.9%.

After heat treatment, the microstructure of the alloy crept for 283 h up to fracture at 650 °C/1034 MPa is shown in Fig. 4, which indicates that the deformation mechanism of alloy during creep is dislocations slipping in the matrix and forming the stacking fault as marked by the arrow; thereinto, the morphology of dislocations shearing the stacking fault stripes is marked by the fine arrow in Fig. 4(a). It is thought through analysis that two sides in the stacking fault exist two (1/3)(112) super-shockleys partials which originates from the decomposition of 110 super-dislocation [28]. In another local region, the boundary in the alloy is marked by the short arrow in Fig. 4(b); in the left side of the boundary, several dislocation bunches with parallel feature slipping in the matrix are

Download English Version:

<https://daneshyari.com/en/article/1575059>

Download Persian Version:

<https://daneshyari.com/article/1575059>

[Daneshyari.com](https://daneshyari.com)